Applied Radiation and Isotopes 159 (2020) 109089

Contents lists available at ScienceDirect

Applied Radiation and Isotopes

journal homepage: http://www.elsevier.com/locate/apradiso

# Triple-sensitivity high-spatial-resolution X-ray computed tomography using a cadmium-telluride detector and its beam-hardening effect

Sohei Yoshida [a], Eiichi Sato [b,*], Yasuyuki Oda [b], Kunihiro Yoshioka [a], Hodaka Moriyama [c], Manabu Watanabe [c]

[a] Department of Radiology, School of Medicine, Iwate Medical University, 2-1-1 Idaidori, Yahaba, Iwate, 028-3694, Japan
[b] Department of Physics, Iwate Medical University, 1-1-1 Idaidori, Yahaba, Iwate, 028-3694, Japan
[c] Department of Surgery, Toho University Ohashi Medical Center, 2-22-36 Ohashi, Meguro, Tokyo, 153-8515, Japan

ARTICLE INFO

*Keywords:*
X-ray CT
Low-noise CdTe detector
Triple amplifier
Triple sensitivity
Triple energy
High spatial resolution

ABSTRACT

To observe blood vessels at high contrasts, we constructed a first-generation triple-sensitivity X-ray computed tomography (TS-CT) scanner using a cadmium-telluride (CdTe) detector and a triple-amplifying system. X-ray photons are absorbed by the CdTe crystal, and the electric charges produced by photons are converted into voltages using a current-to-voltage (I–V) amplifier, and the I–V output is amplified by a voltage-to-voltage (V–V) amplifier. The V–V output 1 is sent to a dual V–V amplifier through a 5.0-m-length coaxial cable and amplified to two-different outputs of 2 and 3. The three outputs 1–3 are sent to a personal computer through an analog-to-digital converter to reconstruct three tomograms simultaneously. In the TS-CT, the scattering photons from the object are extremely reduced using a 0.5-mm-diameter lead pinhole behind the object. The translation and rotation steps were 0.1 mm and 0.5°, respectively, and the spatial resolutions were 0.25 × 0.25 $mm^2$. The scanning time was 19.6 min, and blood vessels were visible using gadolinium contrast media. In particular, the effective photon energy increased with increasing amplification factor of the amplifier caused by beam hardening of the object.

## 1. Introduction

Generally, quasi-monochromatic X-ray imaging is performed using K-series characteristic X-rays (K photons), and a cerium X-ray generator (Sato et al., 2004) has been developed to perform enhanced K-edge angiography using iodine contrast media. The cerium-K photons are absorbed effectively by iodine-based contrast media, and fine blood vessels are observed at a high contrast. On the other hand, gadolinium (Gd) contrast media can be used to image blood vessels, and Gd-K-edge radiography has been carried out using K photons from tantalum (Sato et al., 2005) and tungsten (Sato et al., 2008) targets.

The K-edge CT can also be performed using photon-counting energy-dispersive CT (ED-CT) using a high-energy-resolution CdTe detector, and several first-generation ED-CT scanners have been developed (Matsukiyo et al., 2017; Sato et al., 2017; Moriyama et al., 2019). Subsequently, CdTe-array detectors (Feuerlein et al., 2008; Ogawa et al., 2012) have been developed to construct preclinical ED-CT scanners to perform K-edge CT.

Using visible- and near-infrared-ray photons, we usually use high-sensitivity CT (Sato et al., 2018) since these photons are absorbed easily by biomedical objects. In this regard, although the X-ray photons easily penetrate the objects, the high-sensitivity CT can be applied to image thick object. In addition, it is well known that the X-ray beam hardening is caused by the low-energy-photon absorption by the object when using entire photons.

In the present research, our major objectives are as follows: to develop a triple-amplifying system for the room-temperature CdTe detector, to perform triple-sensitivity CT, to reduce the translation step, to improve the image quality by reducing the pixel dimensions for image reconstruction, and to carry out triple-energy CT utilizing the beam-hardening by the object without any image processing. Therefore, we developed a triple-sensitivity CT (TS-CT) scanner and confirmed the significant contrast variations with changes in the amplification factor.

* Corresponding author.
*E-mail address:* dresato@iwate-med.ac.jp (E. Sato).

https://doi.org/10.1016/j.apradiso.2020.109089
Received 12 September 2019; Received in revised form 26 December 2019; Accepted 19 February 2020
Available online 22 February 2020

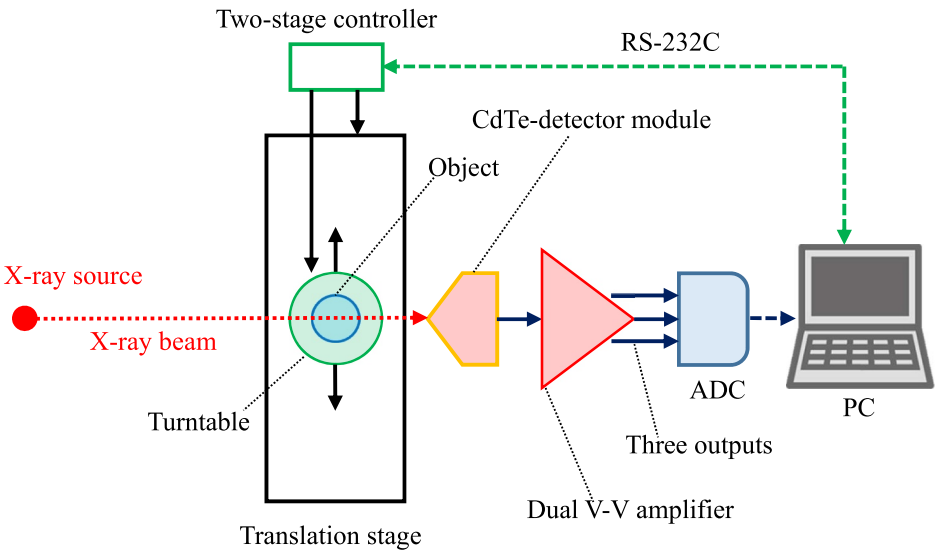


**Fig. 1.** Main components of the TS-CT scanner. The primary X-ray photons penetrating through the object are detected using the CdTe-detector module, and the three outputs including the module are produced using the dual V–V amplifier and are input to the PC through the ADC. The translation stage and turntable are driven by a two-stage controller.

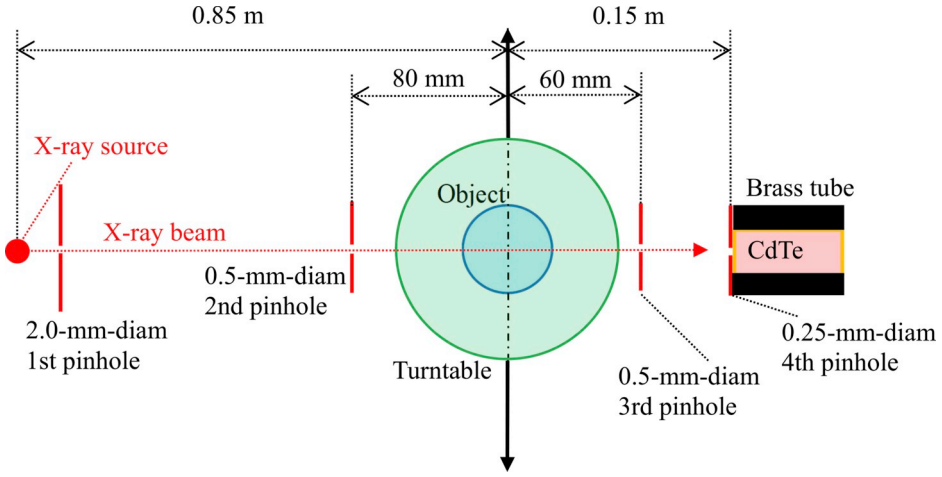


**Fig. 2.** Experimental arrangement of the TS-CT scanner around the object. The X-ray source and the CdTe-detector module are fixed, and the turntable is set on the translation stage. The CT is accomplished by repeating the reciprocal movement of object on the turntable and the rotation of object by the turntable. The line beam is formed using the first and second pinholes placed in front of the object. The scattering photons are reduced using the third pinhole behind the object, and the spatial resolution is determined using the fourth pinhole attached to the detector.

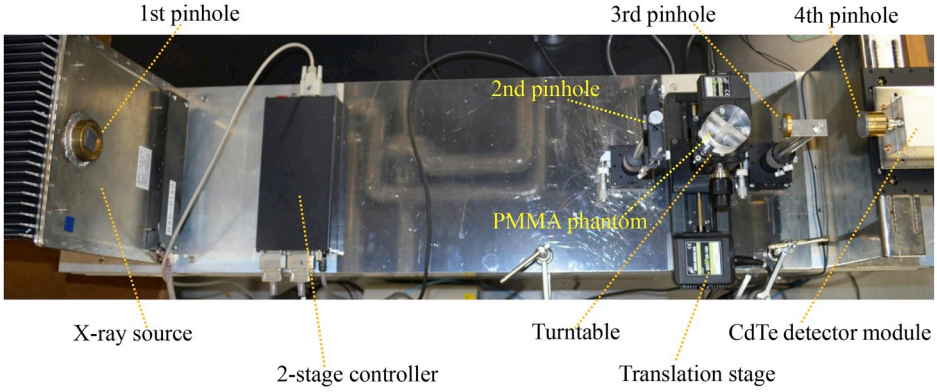


**Fig. 3.** Main components of the TS-CT scanner constructed on the surface plate. The X-ray source was fixed, and the detector was aligned with the X-ray beam passing through the center of the turntable using the x stage. Subsequently, the second and third pinholes were aligned with the beam using the x stages and the helical-rod stands.

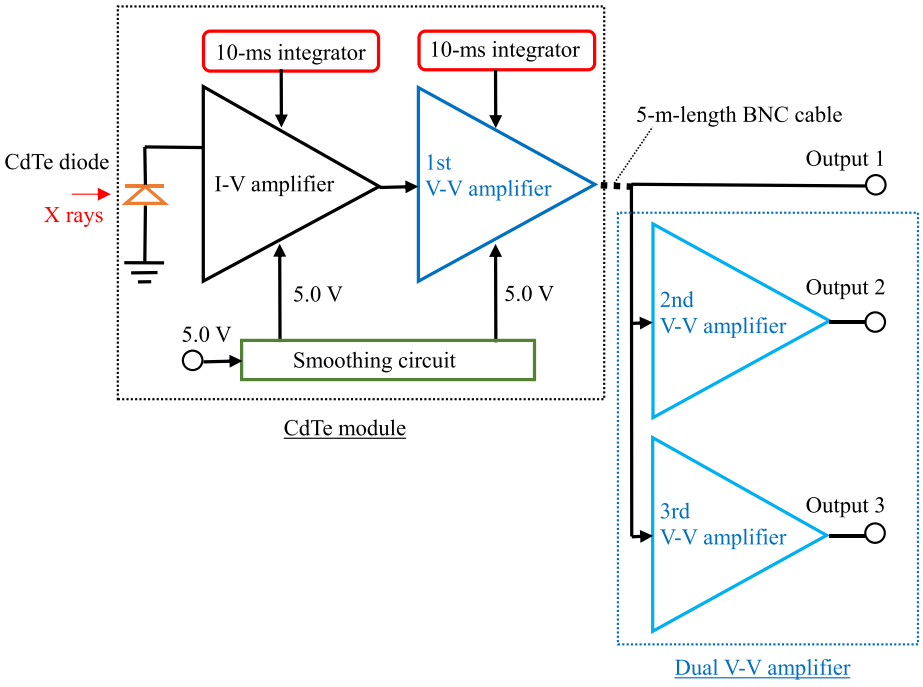


**Fig. 4.** Block diagram of the triple-amplifying system using the CdTe-detector module, a 5.0-m-length coaxial cable, and the dual V–V amplifier. The current flowing through the CdTe diode is converted into voltage and amplified using I–V and V–V amplifiers in the module, and the output voltage is maximized to 5.0 V by regulating the tube current to 1.06 mA. The module output is sent to the dual amplifier, and the three outputs including the module output are produced using the dual amplifier.

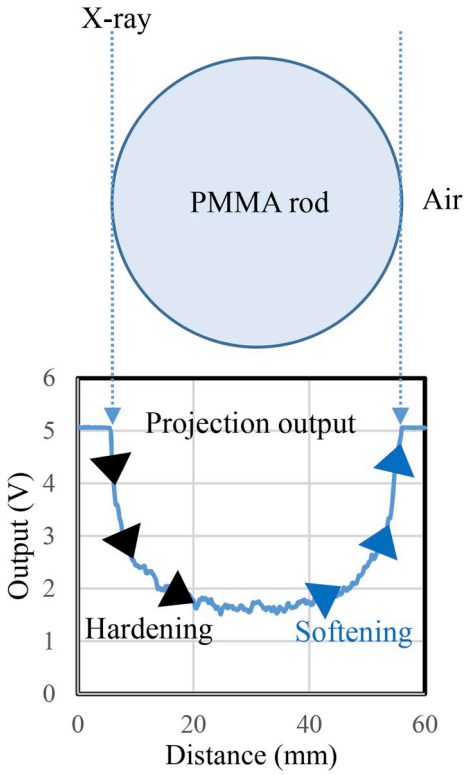


**Fig. 5.** Relationship among the X-ray irradiation, the photon absorption by the 50-mm-diameter PMMA rod, and the projection output from the CdTe-detector module. Low-energy photons are absorbed by the object first, and the high-energy photons penetrate the object. Therefore, the beam hardening is caused by the object.

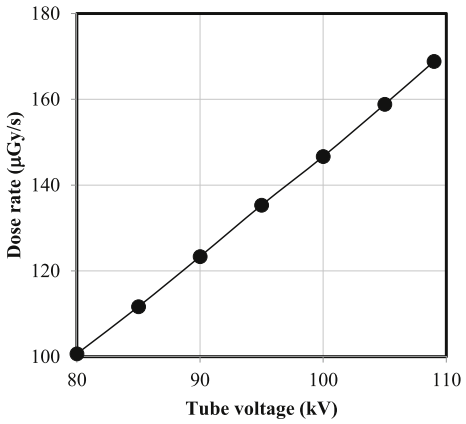


**Fig. 6.** X-ray dose rate at 0.85 m from the X-ray source and a tube current of 1.06 mA.

## 2. Experimental methods

### 2.1. TS-CT

The main components of the TS-CT scanner are presented in Fig. 1. An object is exposed to the X-ray photons produced from the X-ray generator (R-tec, RXG-0152), and the CdTe-detector module detects the primary photons. The electric charges produced in the CdTe are converted into voltages and amplified using current-to-voltage (I–V) and voltage-to-voltage (V–V) amplifiers in the CdTe module, and the module output is input to a dual V–V amplifier. The three outputs including the module output are input to an analog-to-digital converter (ADC; Contec, AI-1608AY-USB), and the ADC output is sent to a personal computer (PC). Both the X-ray source and the CdTe module are fixed, and the object on a turntable (Siguma Koki, SGSP-60YAW-OB) is placed on a translation stage (Siguma Koki, SGSP-26-100). The translation stage and the turntable are driven by a two-stage controller (Siguma Koki, SHOT-602). The object on the turntable rotates by 0.5° between translations, and the velocity and stroke of the translation are 25 mm/s and 60 mm,

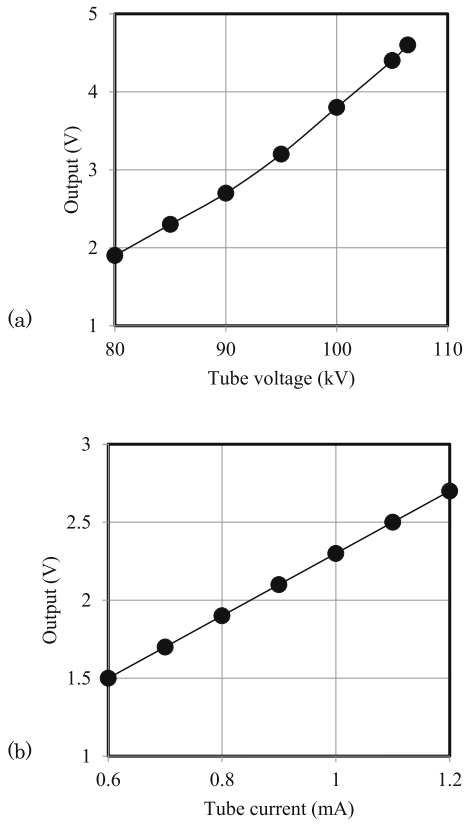


**Fig. 7.** CdTe-module outputs. (a) The output increased with increases in the tube voltage at a constant tube current of 0.80 mA, and (b) the output was in proportion to the tube current at a constant tube voltage of 80 kV.

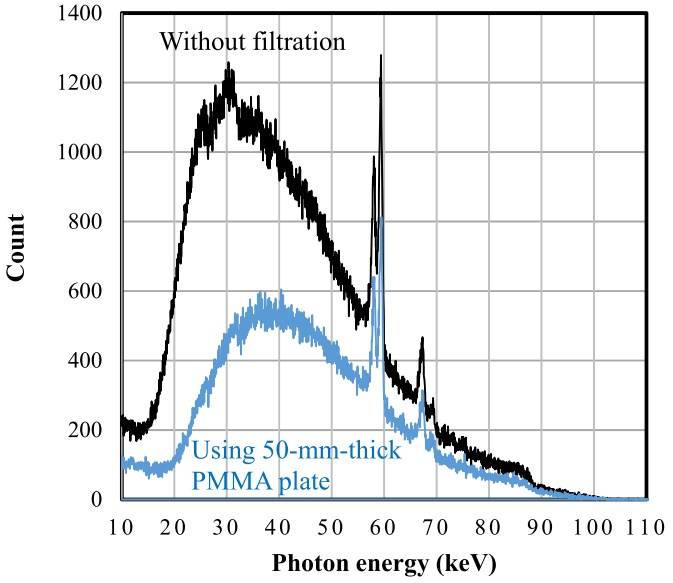


**Fig. 8.** Variations of X-ray spectra with the beam hardening at a tube voltage of 100 kV. Low-energy photons were absorbed by a 50-mm-thickness PMMA plate.

respectively.

Figs. 2 and 3 shows the experimental setup around the object. The X-ray-source-to-detector distance is 1.00 m, and the turntable-center-to-detector distance is 0.15 m. In the scanner, we used four 3.0-mm-thickness Pb pinholes, and the outer diameters of the first to fourth pinholes are 50, 30, 30 and 30 mm, respectively. The line beam is roughly formed using the 2.0-mm-diameter first pinhole, and the beam diameter is reduced by the 0.5-mm-diameter second pinhole in front of the object. Subsequently, the scattered photons are reduced using the 0.5-mm-diameter third pinhole behind the object, and the spatial resolution is determined by the 0.25-mm-diameter fourth pinhole attached to the detector. Therefore, almost only the primary photons can be detected. While performing the tomography, the reciprocating translation and rotation are repeated.

The TS-CT scanner was constructed on a surface plate with a 1.0-mm-thick stainless-steel plate (SUS304). In this experiment, the X-ray source was fixed using two bolts, and the detector was aligned with the X-ray beam passing through the center of the turntable using the x stage (Siguma Koki; TASB-601) in a direction perpendicular to the beam. The second and third pinholes were fixed using magnetic bases (Siguma Koki, MB-L65C-M4), and their positions were aligned using x stages (Siguma Koki, TSDT-601S) and helicoid-rod stands (Siguma Koki, RSN-12).

To reconstruct tomograms, the convolution back-projection method with Shepp-Logan function is used, and the ray-sampling translation and rotation are performed in steps of 0.1 mm and 0.5°, respectively. The translating is carried out smoothly by reading the instantaneous values every 10 ms, and the scanning time is proportional to the total rotation angle of 180° and is 19.6 min.

### 2.2. CdTe-detector module

Fig. 4 shows the block diagram of the CdTe detector module and the dual V–V amplifier. In the module, the current flowing through the CdTe diode is converted into voltage using the I–V amplifier with a 100-MΩ resistor for producing outputs and a 10-ms-time-constant integrator for smoothing, and the I–V output is input to the $1.0 \times 10^3$-time V–V amplifier. Subsequently, the V–V output is sent to the dual V–V amplifier through a 5.0-m-length coaxial cable and input to the ADC directly. In addition, the V–V output is amplified by two V–V amplifiers, and the two outputs are also sent to the ADC.

### 2.3. Measurements of X-ray dose rate and amplifier-module output

The X-ray dose rate was measured using a dosimeter (Toyo Medic, RAMTEC 1000 plus) with an ionization chamber (Scanditronix, DC300) to calculate the incident dose for the object. The chamber was placed 0.85 m from the X-ray source without filtration at the center of turntable and a tube current of 1.06 mA.

The electric charge produced in the CdTe crystal is proportional to the photon energy, and we measured the output from the module with changes in the tube voltage and current using a digital voltmeter.

### 2.4. Measurement of X-ray spectra

The X-ray spectra were measured using a CdTe detector system (Amptek, XR-100T) and a 0.5-mm-diameter Pb pinhole. The photon energy was determined by the two-point calibration using $K\alpha_1$ photons of tungsten and iodine.

### 2.5. Principle of beam hardening

The relationship among the X-ray irradiation, the X-ray absorption by a 50-mm-diameter polymethyl methacrylate (PMMA) rod, and a projection output is shown in Fig. 5. The X-ray photons are absorbed by the PMMA, and the real projection output is shown in the figure for reference. It is well known that the low-energy photons are absorbed first, and the high-energy photons penetrate the PMMA rod. Therefore, the effective energy of the projection output increases with increasing the amplification factor at a constant maximum output.

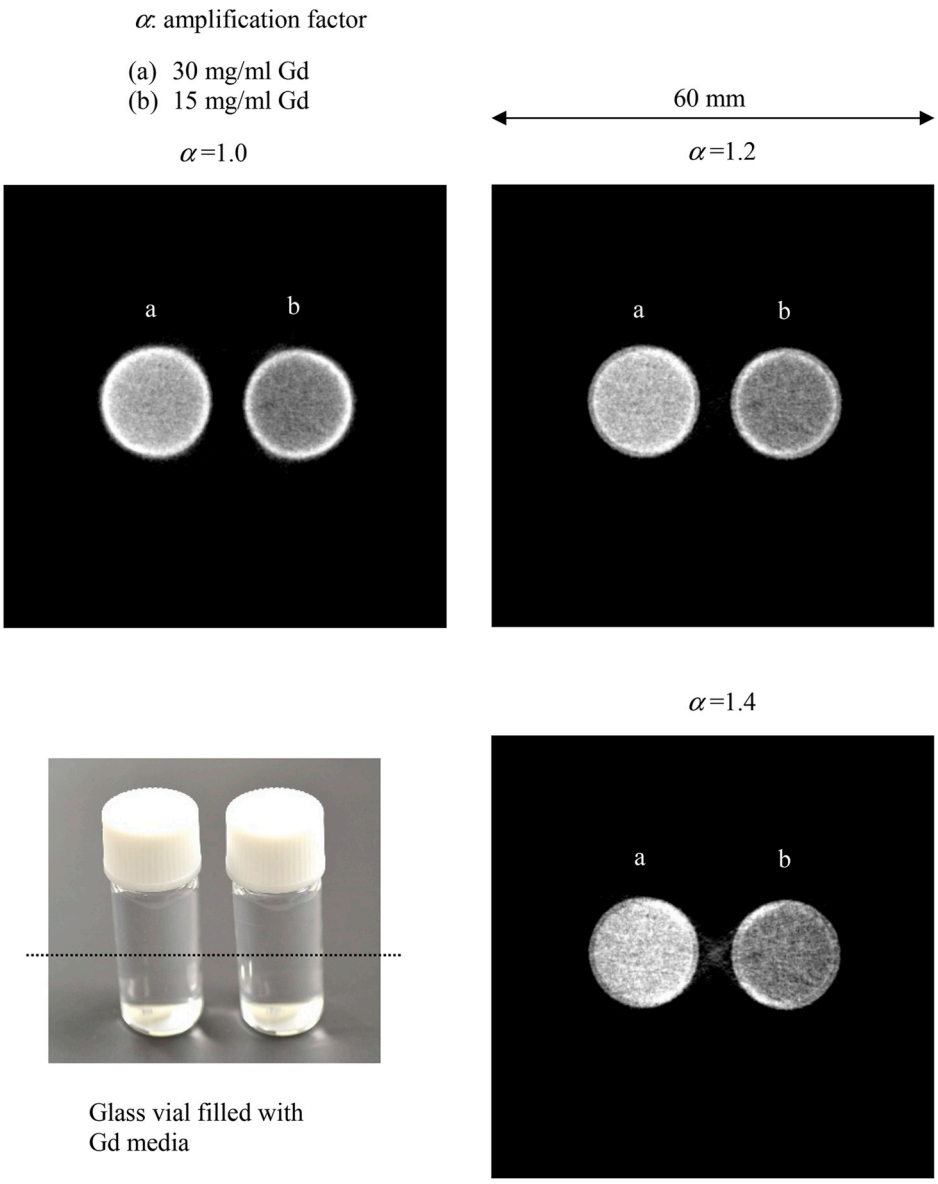


**Fig. 9.** Tomography of two glass vials filled with Gd media of two different Gd concentrations of 15 and 30 mg/ml. The gray-value-density difference between the two media increased with increasing amplification factor.

### 2.6. Real animal phantom

In the TS-CT, a real rabbit-head phantom was used. This phantom was made approximately 20 years ago, and the operation on animals was performed according to the animal experiment guidelines in Iwate Medical University (28-014).

## 3. Results

### 3.1. X-ray dose rate and amplifier-module output

Fig. 6 shows X-ray dose rate measured at the center of the turntable. The X-ray dose rate increased when the tube voltage was increased at a tube current of 1.06 mA. At a tube voltage of 100 kV, the X-ray dose rate had a value of 155 μGy/s.

The amplifier-module outputs are shown in Fig. 7. At a constant tube current of 0.80 mA, the output increased with increasing tube voltage. On the other hand, the output was proportional to the tube current at a constant tube voltage of 80 kV.

### 3.2. X-ray spectra

X-ray spectra at a tube voltage of 100 kV are shown in Fig. 8. Without filtration, bremsstrahlung peak energy was approximately 30 keV, and sharp tungsten K lines were observed. Subsequently, the bremsstrahlung-peak energy shifted to approximately 37 keV by the insertion of a 50-mm-thickness PMMA plate. Therefore, the effective energy also shifted to high energy when X-ray photons are absorbed by the object.

### 3.3. Tomography

Tomography was accomplished at a tube voltage of 100 kV and a current of 1.06 mA. The tomograms were reconstructed using the digital projection outputs from the 16-bit ADC and finally converted into JPEG files, and the maximum and minimum gray-value densities are defined as white (255) and black (0), respectively. At the constant maximum output of 5.0 V, the output is proportional to the amplification factor $\alpha$, and the effective energy increases with increasing $\alpha$.

Fig. 9 shows tomography of two glass vials filled with Gd

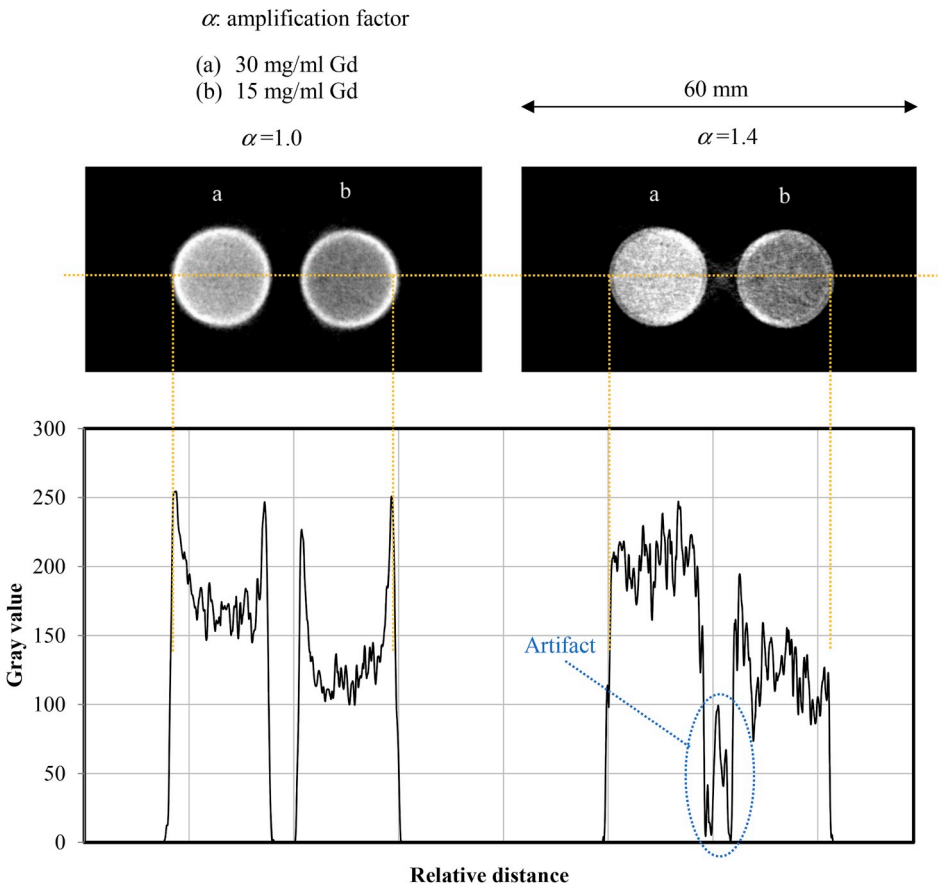


**Fig. 10.** Image-density analysis of glass vials filled with Gd media in Fig. 9. At an $\alpha$ of 1.0, the glass walls were visible. With increases in the amplification factor to 1.4, although the image density difference between media increased, the glass walls were not visible.

(meglumine gadopentetate) media of two different Gd concentrations of 15 and 30 mg/ml. When the amplification factor is increased, the image density difference increased. At an $\alpha$ of 1.4, the artifact between the two vials was observed.

The gray-value density analysis of the two glass vials in Fig. 9 is presented in Fig. 10. At an $\alpha$ of 1.0, two vials were observed at high contrasts, and glass walls were visible. With increases in the factor to 1.4, the image-density difference between the two media increased, and the glass walls were not visible.

Fig. 11 shows the tomography of a PMMA phantom with four holes filled with Gd medium of 30 mg/ml. When the amplification factor was increased, the image density of PMMA body substantially decreased, and the image density of the medium maximized at an $\alpha$ of 1.8.

The tomography of a rabbit-head phantom is shown in Fig. 12. The blood vessels were filled with gadolinium oxide microparticles with diameters ranging from 1 to 10 μm. On the other hand, radiography was performed for reference using a flat-panel detector (FPD; Rad-icon Imaging 1024EV) to display a cross section. At an $\alpha$ of 1.0, the image densities of muscle and bone were high, and the image contrast of the blood vessels was low. With increasing the amplification factor, the image densities of the muscle and bone decreased, and the vessels were observed at a high contrast. At factors beyond 2.0, tomograms were equivalent to those obtained utilizing photon-counting Gd-Kedge CT.

## 4. Discussion

We performed the first-generation TS-CT using a high-sensitivity CdTe-detector module and a dual amplifier (Table 1). In this TS-CT, we reduced the translation step from 0.25 to 0.1 mm to improve the image quality. In addition, the quality could be improved by decreasing the rotation step from 1.0 to 0.5°.

The principle of TS-CT is quite simple, and it is well known that the beam hardening is caused by the X-ray-photon absorption of objects when using entire photons from the X-ray source. In this experiment, we confirmed the strong contrast variations with changes in the amplification factor.

Since the CdTe detector with amplifiers was very sensitive to ambient noises, we reduced the electric noises using an aluminum-shielding case. Subsequently, we used the two 10-ms-time-constant integrators to reduce the noises produced from the I–V and V–V amplifiers. The CdTe-module outputs were much higher than the noises, and the module was easily connect to the dual amplifier using the coaxial cable. In addition, the tube current was increased to 1.06 mA to reduce the photon-number fluctuation.

The TS system consists of a CdTe module, 5.0-m-length coaxial cable and a dual V–V amplifier. Using the dual amplifier, it is easy to produce two projection outputs at amplification factors beyond 1.0. In addition, the projection outputs can also be calculated using a digital amplifier, and dual-, triple- and quad-sensitivity CT can easily be performed when enough penetrating photons are obtained.

In the TS-CT, three projection outputs were obtained with changes in the amplification factor, and three-different-energy tomograms were obtained simultaneously without special image processing. To simplify the triple-amplifying system, the digital amplifier might be useful for increasing the effective photon energy of the TS-CT.

For this research, we reduced the pixel dimensions to $0.1 \times 0.1$ mm$^2$ to reconstruct the tomogram. Next, the spatial resolution was determined effectively by the detector-pinhole diameter of 0.25 mm, and the spatial resolutions were approximately $0.25 \times 0.25$ mm$^2$. At the constant pinhole diameter of 0.25 mm and a translation step of 0.1 mm, the

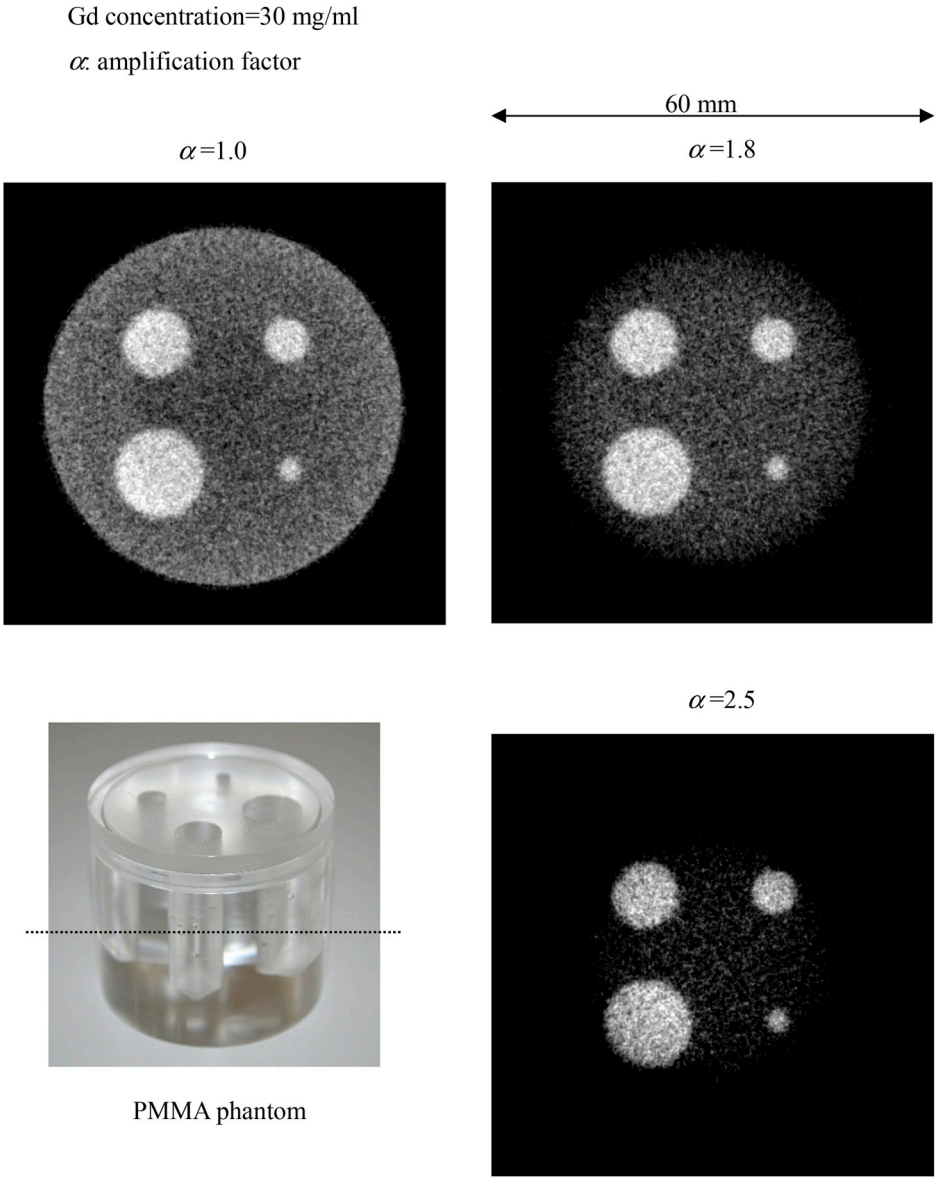


**Fig. 11.** Tomography of the PMMA phantom with four holes filled with Gd medium of 30 mg/ml. With increasing amplification factor, the image density of PMMA body decreased, and the image density of the medium maximized at an $\alpha$ of 1.8.

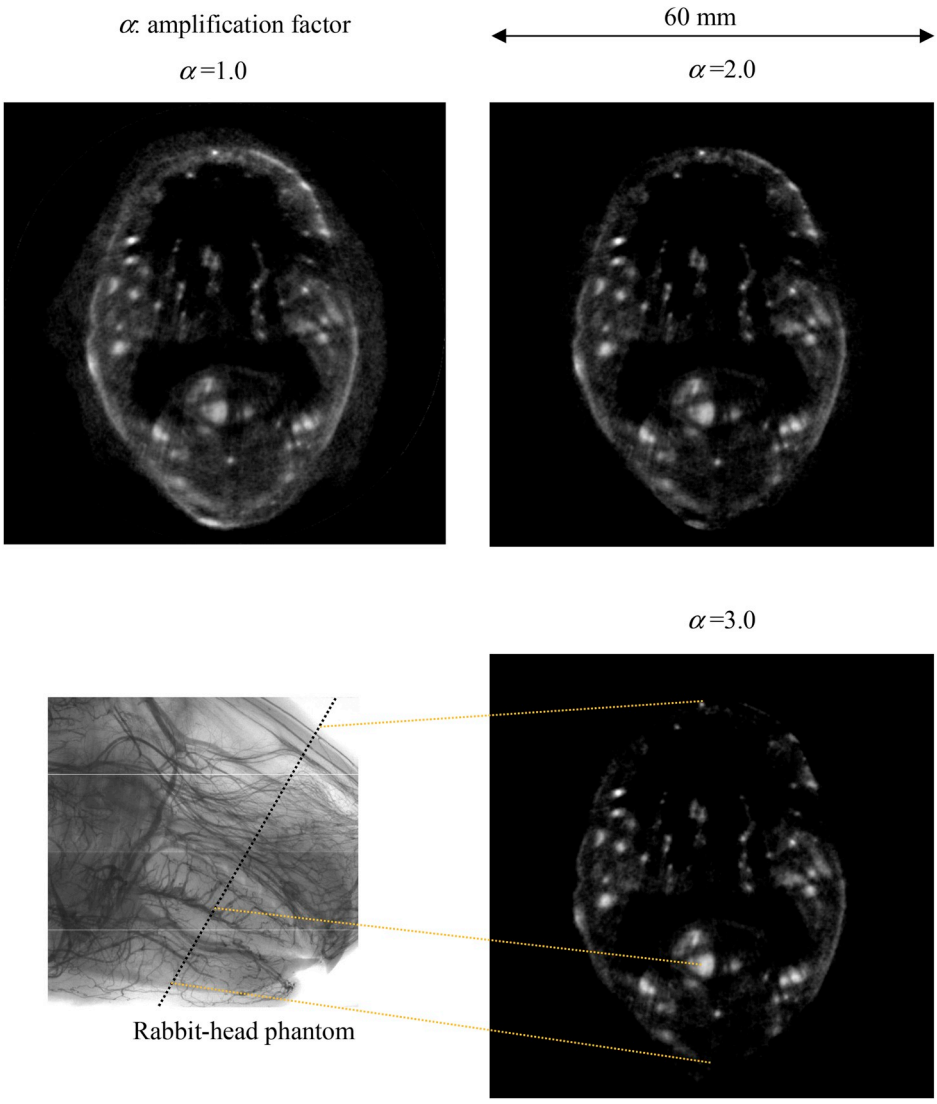


**Fig. 12.** Tomography of a rabbit-head phantom. When increasing the amplification factor, the image densities of muscle and bone decreased, and the image contrast of the blood vessels improved.

**Table 1**
Various TS-CT specifications using the CdTe-detector module. The 0.5-mm-diameter line beam was used to reduce the incident dose and scattering photons from the object. The spatial resolutions were approximately 0.25 × 0.25 $mm^2$, and the scanning time was 19.6 min at a translation step of 0.1 mm, a rotation step of 0.5°, and a total rotation angle of 180°.

| Specifications | |
|---|---|
| Generation type | 1st |
| Beam type | Line |
| Beam diameter (mm) | Approx.0.5 |
| Detector | Room-temperature CdTe |
| Stroke (mm) | 60 |
| Turntable diameter (mm) | 60 |
| Pinhole diameter for detector (mm) | 0.25 |
| Translation velocity (mm/s) | 25 |
| Translation step (mm) | 0.1 |
| Rotation step (°) | 0.5 |
| Total rotation angle (°) | 180 |
| Scanning time (min) | 19.6 |
| Reconstructed pixel dimensions ($mm^2$) | 0.1 × 0.1 |
| Spatial resolutions ($mm^2$) | Approx. 0.25 × 0.25 |
| Incident dose (mGy) | 1.1 |

rotation step should be reduced to 0.25° to improve the image quality. To improve the spatial resolution to approximately 0.1 × 0.1 $mm^2$, a 0.1-mm-focus X-ray tube would be desired.

The object was placed at 0.85 m from the X-ray source, and the dose rate measured was 155 μGy/s at a tube voltage of 100 kV and a current of 1.06 mA. Using the 0.5-mm-diameter line beam, the incident dose is 3.1 μGy at the irradiation spot and a rotation step of 0.5°, since the translating time per 0.5 mm is 20 ms. Thus, the total incident dose at a rotation angle of 180° is roughly calculated as 1.1 mGy. Therefore, the dose increases with increases in the beam diameter, and the diameter should be minimized to 0.25 mm.

## 5. Conclusions

We performed TS-CT using the triple-amplifier system to change the amplification factor of the projection output. In the case where the monochromatic imaging is not desired, the TS-CT is useful for increasing the effective photon energy of CT with increasing the amplification factor when enough photons at high amplification factors are obtained.

## Ethical approval

This article does not contain any studies on animals or human participants.

## Declaration of competing interest

The authors declare no conflict of interest.

## CRediT authorship contribution statement

**Sohei Yoshida:** Visualization, Investigation, Writing - original draft. **Eiichi Sato:** Writing - original draft, Writing - review & editing. **Yasuyuki Oda:** Software. **Kunihiro Yoshioka:** Supervision. **Hodaka Moriyama:** Visualization, Investigation. **Manabu Watanabe:** Supervision.

## Acknowledgments

This work was supported by Grants from Keiryo Research Foundation, Promotion and Mutual Aid Corporation for Private Schools of Japan, Japan Science and Technology Agency (JST), and JSPS KAKENHI (17K10371, 17K09068, 17K01424, and 17H00607). This was also supported by a Grant-in-Aid for Strategic Medical Science Research (S1491001 and 2014–2018) from the Ministry of Education, Culture, Sports, Science and Technology of Japan.

## Appendix A. Supplementary data

Supplementary data to this article can be found online at https://doi.org/10.1016/j.apradiso.2020.109089.

## References

Feuerlein, S., Roessl, E., Proksa, R., Martens, G., Klass, O., Jeltsch, M., Rasche, V., Brambs, H.J., Hoffmann, M.H.K., Schlomka, J.P., 2008. Multienergy photon-counting K-edge imaging: potential for improved luminal depiction in vascular imaging. Radiology 249, 1010–1016.

Matsukiyo, H., Sato, E., Oda, Y., Ishii, T., Yamaguchi, S., Sato, Y., Hagiwara, O., Enomoto, T., Watanabe, M., Kusachi, S., 2017. Investigation of quad-energy photon counting for X-ray computed tomography using a cadmium telluride detector. Appl. Radiat. Isot. 130, 54–59.

Moriyama, H., Watanabe, M., Kusachi, S., Oda, Y., Sato, E., 2019. Low-dose low-scattering X-ray computed tomography with high-spatial-energy resolutions using a cooled cadmium telluride detector. Ultramicroscopy 199, 62–69.

Ogawa, K., Kobayashi, T., Kaibuki, F., Yamakawa, T., Nagano, T., Hashimoto, D., Nagaoka, H., 2012. Development of an energy-binned photon-counting detector for X-ray and gamma-ray imaging. Nucl. Instrum. Methods A 664, 29–37.

Sato, E., Tanaka, E., Mori, H., Kawai, T., Ichimaru, T., Sato, S., Takayama, K., Ido, H., 2004. Demonstration of enhanced K-edge angiography using a cerium target x-ray generator. Med. Phys. 31, 3017–3022.

Sato, E., Hayasi, Y., Kimura, K., Tanaka, E., Mori, H., Kawai, T., Inoue, T., Ogawa, A., Sato, S., Takayama, K., Onagawa, J., Ido, H., 2005. Enhanced K-edge angiography utilizing tantalum plasma x-ray generator in conjunction with gadolinium-based contrast media. Jpn. J. Appl. Phys. 44, 8716–8721.

Sato, Y., Sato, E., Ehara, S., Enomoto, T., Tanaka, E., Mori, H., Kawai, T., Ogawa, A., Sato, S., Onagawa, J., 2008. Magnification K-edge angiography utilizing 100-μm-focus tungsten tube and gadolinium-based contrast media. Jpn. J. Appl. Phys. 47, 4772–4776.

Sato, E., Kosuge, Y., Yamanome, H., Mikata, A., Miura, T., Oda, Y., Ishii, T., Hagiwara, O., Matsukiyo, H., Watanabe, M., Kusachi, S., 2017. Investigation of dual-energy X-ray photon counting using a cadmium telluride detector with dual-energy selection electronics. Radiat. Phys. Chem. 130, 385–390.

Sato, Y., Takaoka, A., Sato, T., Sato, E., Oda, Y., Yoshida, S., Moriyama, H., Hagiwara, O., Matsukiyo, H., Enomoto, T., Watanabe, M., Kusachi, S., 2018. 850-nm-peak high-sensitivity near-infrared-ray computed tomography scanner in the living-body window. Health Technol. 8, 205–210.